



A cost-effective device and methodology to compute aquifer transmissivity and piezometry from free-flowing artesian wells

Alix Toulhier^{1,2,3} · Patrick Lachassagne³ · Heru Hendrayana⁴ · Arif Fadillah⁵ · Hervé Jourde³

Received: 16 September 2021 / Accepted: 2 June 2022 / Published online: 19 July 2022
© The Author(s) 2022

Abstract

Artesian aquifers offer interesting opportunities for water supply by providing a low-vulnerability groundwater resource that is easily abstracted without any installation of pumps or power supply costs. However, hydraulic tests are challenging to perform, notably where the piezometric head is above ground level with free-flowing wells not equipped with valves and open for years. This paper describes a low-cost, easy to reproduce and adaptable device, the free-flowing artesian well device (FFAWD), which is mainly designed with a set of PVC tubes equipped with a pressure probe and a valve. This device is used to perform hydraulic tests on free-flowing artesian wells, to measure the piezometric head of the aquifer and to compute its transmissivity. The practical use of the FFAWD is described and a method is proposed to compute the piezometric head and the transmissivity of the aquifer from this data set (free-flowing well discharge and pressure increase measurements) with any adapted analytical solution, using the Houpeurt-Pouchan method. Artefacts such as post-production effects, surge effects, and the impact of a leaky well are identified to avoid any misinterpretation. The FFAWD was applied to the volcano-sedimentary artesian plain of Pasuruan (Indonesia). The advantages and limitations of using the device, along with the interpretation methodology, are also discussed.

Keywords Equipment/field technique · Aquifer testing · Hydraulic properties · Free-flowing artesian well device · Indonesia

Introduction

Artesian conditions develop where the hydraulic head of an aquifer is higher than the topographic surface, allowing the free-flow of groundwater through artesian wells (and/or springs). Large artesian systems are widespread, such as the Great Artesian Basin in Australia (Flook et al. 2020; Habermehl 2020), the Dakota Sandstone in the USA (Meinzer and Hard 1925), and the Ordos Plateau in northwestern China (Jiang et al. 2018). Smaller volcanic systems also display artesian conditions, such as the Honolulu artesian basin in Hawaii (USA) (Wentworth 1951) and the volcano-sedimentary aquifer of Pasuruan in Indonesia (Toulhier et al. 2019). Such artesian systems are of great interest insofar as the groundwater withdrawal does not require any pump installations or incur power supply costs. This is important in developing countries, notably where groundwater is used by low-income farmers (Khasanah et al. 2021). Moreover, these aquifers, where they are confined by an impervious layer, often provide very high-quality groundwater (in terms of microbiology and anthropogenic contaminants) due to the confined conditions.

✉ Alix Toulhier
alix.toulhier@univ-reunion.fr

Patrick Lachassagne
patrick.lachassagne@umontpellier.fr

Heru Hendrayana
heruha@ugm.ac.id

Arif Fadillah
arif.fadillah@danone.com

Hervé Jourde
herve.jourde@umontpellier.fr

¹ Université de Paris, Institut de physique du globe de Paris, CNRS, F-75005 Paris, France

² Laboratoire GéoSciences Réunion, Université de La Réunion, F-97744 Saint Denis, France

³ HSM, Univ Montpellier, CNRS, IMT, IRD, Montpellier, France

⁴ Geological Engineering Department, Universitas Gadjah Mada, Yogyakarta, Indonesia

⁵ Danone Aqua Head Quarter, HR Rasuna Said Street, Jakarta, Kuningan Timur, Indonesia

Confined aquifers have been surveyed and studied in several places around the world for a long time, at least as early as the 19th century, notably the water wells drilled in the Artois region of the Paris Basin (France) from which the term “artesian” is derived (Margat et al. 2013). However, the term “artesian” may cause confusion since, with proper topographic undulation, flowing artesian wells can also develop in an unconfined aquifer (Jiang et al. 2020). Freeze and Cherry (1979) identified two mechanisms for the existence of flowing artesian wells which were named “geologically controlled” and “topographically controlled” (see Fig. 1). This study particularly focuses on the geologically controlled conditions related to a confined aquifer configuration (i.e. artesian aquifer). Accordingly, the term “free-flowing artesian well (FFAW)” is used in this paper.

Several studies, some including hydraulic tests, have demonstrated the elasticity and deformation properties of water-bearing layers in artesian aquifers (Meinzer 1928; Thompson 1929). Other studies have pointed out the complexity of such aquifers regarding the transmission of pressure changes (Legette and Taylor 1934; Versluys 1930) and the rate of spreading of the depression cone (Lohman 1965). However, hydrodynamic studies of artesian systems have mostly focused on only a few free-flowing artesian wells (e.g. in the Table Mountain Group aquifer in South Africa (Lin 2007), the Honolulu artesian basin in Hawaii (Nichols et al. 1996), the Dakota Sandstone in the USA (Meinzer and Hard 1925), and the Ordos Plateau in northwestern China (Wang et al. 2015). A better understanding of such aquifer systems needs a basin-scale hydrogeological characterization that can be undertaken using low-cost and easy to implement devices and methods.

Since the 1960s, several devices for flowing wells have been designed, such as the photographic method with a camera and manometer (Wyrick and Floyd 1961) or use of an ink-well mercury gage for water head monitoring (Lohman 1965). A more accurate device was proposed by Oberlander and Almy (1979), using an ultrasonic flowmeter. Recently, a device was designed by Sun and Xu (2014), integrating an ultrasonic flowmeter and pressure transmitter, and electrical conductivity (EC) and pH probes, all with connections to a data logger requiring an external power supply. Despite the progress in such devices, their use remains complex and laborious in remote locations lacking a power supply or inaccessible

by car, for instance in agricultural areas with paddy fields. In addition, in some developing countries, the poor design of the well heads does not allow the use of classic devices such as ink-well manometers or any other valving equipment at the well head (Khasanah et al. 2021) as the well head will not resist the so-created pressure. Adding a length of transparent glass tubing with graduated scale has been a quite common practice to visualize and measure the piezometric level at flowing wells since Jacob and Lohman (1952). To date, no research has been published on a more sophisticated version of such devices. Therefore, this paper presents a new device that can be adapted for a wide roll-out on numerous free-flowing wells over a short period of time, notably during piezometric surveys.

This study proposes (i) a simple device and method, both cost-effective and easy to implement, without any need for an external power supply, and (ii) a data interpretation methodology, to compute the transmissivity of the aquifer and to access the piezometric head of free-flowing artesian wells.

This method is applied to the artesian volcano-sedimentary aquifer of Pasuruan, located at the foot of the Bromo-Tengger volcano (East Java, Indonesia), in order to draw its piezometric map, and to characterize its transmissivity.

The advantages and limitations of using the device, along with the interpretation methodology and the obtained results (piezometry, transmissivity, conceptual model of the aquifer) are discussed.

Methodology

Basic concepts about artesian aquifers

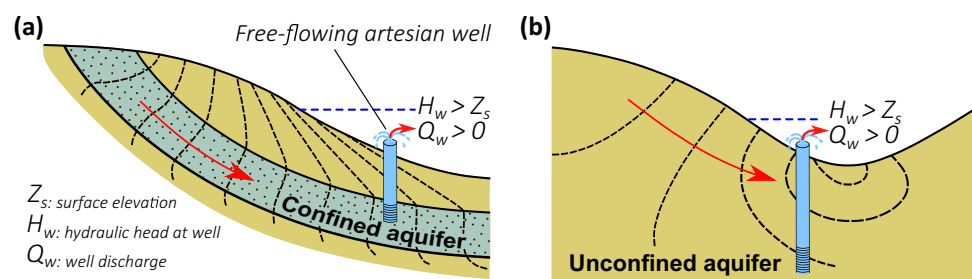
The aim of the device and the associated data interpretation method is to perform measurements that can be used to estimate: (i) the hydraulic head h of the aquifer (Fig. 2), and (ii) the transmissivity T of the aquifer.

As a reminder:

The hydraulic head (h) is defined according to the Bernoulli theorem (Banton and Bangoy 1997), as follows:

$$h = \frac{u^2}{2g} + \frac{P}{\rho g} + z \quad (1)$$

Fig. 1 **a** Geologically-controlled and **b** topographically-controlled free-flowing artesian wells (modified from Jiang et al. 2020)



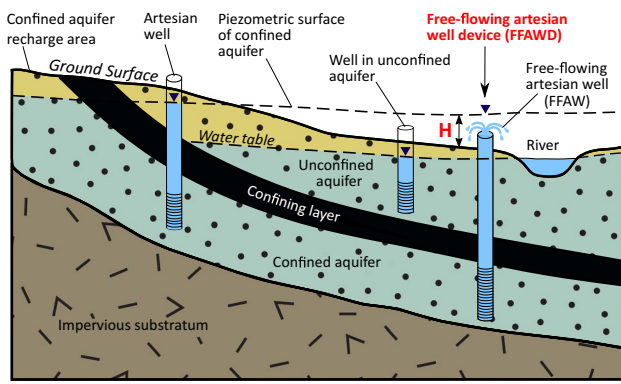


Fig. 2 Conceptual model and technical terms for geologically-controlled confined aquifers, and unconfined aquifers (modified from Chen et al. 2018)

where:

- h piezometric head of the aquifer (m)
- u fluid velocity (m s^{-1})
- P water pressure at the measurement location (kPa), not taking into account the atmospheric pressure (water pressure minus atmospheric pressure)
- ρ volumetric mass of water ($\times 10^3 \text{ kg m}^{-3}$ in standard conditions)
- g acceleration due to gravity (9.81 m s^{-2})
- z elevation above a given datum (m)

In porous media, the fluid velocity is very slow, allowing one to ignore the kinetic energy term ($\frac{u^2}{2g}$), so the hydraulic head (h) can be simplified by the piezometric head (H) given by the following equation (De Marsily 1986):

$$H = \frac{P}{\rho g} + z \quad (2)$$

A free-flowing artesian well (FFAW) has a piezometric head H that is higher than the topographic surface or, rather, higher than the top of the well head (WMO, W. M. O, and UNESCO 2012; Chen et al. 2018). However, an artesian well is not necessary flowing at the surface as illustrated in Fig. 2.

In the following parts of this paper, the developed device will be referred to as a “free-flowing artesian well device” (FFAWD).

Design of the free-flowing artesian well device (FFAWD)

The principle of the measurement method is to install the device on the well head (Fig. 3a), allowing the pressure to increase inside the device and be monitored. The device is

built up as follows, from bottom to top (with spare parts respectively labeled from (I) to (V) in Fig. 3 c):

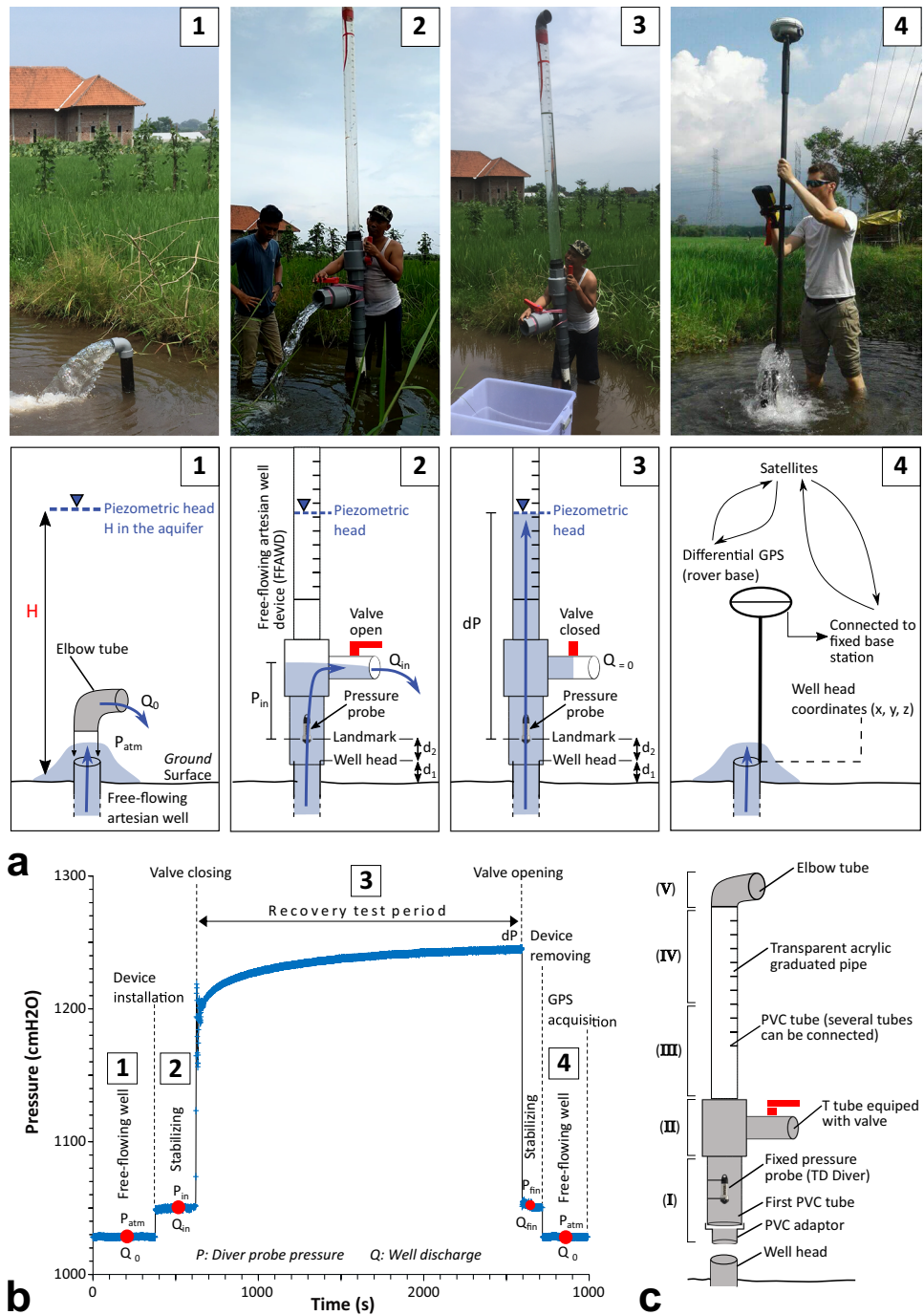
- A PVC tube (labeled (I)) whose base diameter can be changed in the field to adapt to the well head diameter. It can also be equipped with an elbow tube in case the outlet of the free-flowing well is not vertical. This first tube comprises a smaller tube which is fixed inside to install and secure the pressure probe. Note that for pressure probes not compensated for atmospheric pressure, a barometer probe might be useful for such a compensation; however, as these measurements are performed during a short period of time (usually less than one hour), during which atmospheric pressure changes are expected to be very low, this is not mandatory. The pressure probe is easy to extract from the device, to download data when the measurement process is over, and is also easy to reinsert.
- A T tube (II) whose horizontal outlet is equipped with a valve.
- The vertical outlet (III) of the T tube is equipped by successively adding tube sections depending on the H . Then, a transparent acrylic graduated pipe (IV) is connected with a last tube section, open at the top, which allows observation of the water level during the test. The top of this transparent pipe is equipped with an elbow outlet (V) to redirect the water flow if H is higher than the measuring device, to avoid wetting the technicians as well as to enable discharge measurements.

This study used a Van Essen TD-Diver pressure probe for water levels ranging from 0 to 10 m, with a ± 0.5 cm precision and a resolution of 0.06 cm. The pressure was recorded at 1 s intervals. The PVC and acrylic pipes are 100 mm (4 inches) in diameter. Acrylic/PVC tubes, up to 6 m long, were connected to each other to measure high piezometric heads. Only the last tube is composed of a 2 m transparent acrylic pipe. A maximum water level of 8 m above ground surface was measured with this device.

Measurement procedure

First, it is important to select reliable free-flowing artesian wells without any visible leakage between the casing and the ground surface, since grouting can be of poor quality or non-existent in wells owned by farmers with modest means such as in Pasuruan. The wells with a concrete base, satisfactory grouting and a well head in good condition (no corrosion or breaking) were selected in priority. However, as seen later (*Results* section), some tested wells were leaking. It is also recommended to select wells with a vertical, open and straight pipe long enough to connect the device. Wells with a well head diameter less than 7–8 cm (3 inches) are not recommended as they are not strong enough for the device

Fig. 3 **a** Description of the free-flowing artesian well device (FFAWD) and measurement method through steps 1 to 4. **b** Typical pressure data set recorded by the probe over time (test on well n°8). The characteristics of free-flowing well n°8 are described in Table 1. **c** Design of the FFAWD



and may break during the test. A prior manual discharge measurement (Q_0) allows a rough estimate of the number of PVC tubes required for the hydraulic test. Of course, the selected wells should meet the purpose of the study: for instance, a homogeneous spatial distribution to ensure an accurate piezometric map, or locations chosen to characterize the hydrodynamic properties (e.g., T) of various lithological units. Then, the measurement procedure comprises four main steps respectively illustrated in Fig. 3:

Step 1. Discharge measurement: Measurement of the “steady” discharge of the free-flowing well (Q_0). The fitting of an elbow on the vertical pipe improves the accuracy of the flow measurement, even if it may slightly reduce the discharge due to the slight increase of the piezometric head (in this study, the reduction is between 3 and 5%; this point is addressed in the *Discussion* section). The discharge measurement is performed manually with a bucket or any other graduated or gauged collection

container. A 140 L bucket was used in this study. Within the range of the discharge measurement interval (± 0.5 s), the uncertainty on the discharge is between 0.4% and 3%, respectively, for a discharge of about 1 L s^{-1} and 15 L s^{-1} . It is recommended to carry out several discharge measurements to further reduce the uncertainty on the discharge value (3 to 5 measurements at least). The fact that the discharge should be “steady” prior to the test is also addressed in the *Discussion* section.

Step 2. Device installation:

- The setting up and calibration of the pressure probe is carried out before setting it inside the device.
- The device is installed on the well head with the valve open (Fig. 3a).
- After a few minutes of flow stabilization (that can be regularly measured), as there is a change in piezometric head related to installation of the device (P_{in}), a discharge measurement is performed to estimate the “initial” well discharge (Q_{in}). As written above, it is recommended to perform several discharge measurements to reduce the uncertainty on this data.
- The height parameters of the device are measured: at least, height from ground surface to well head (d_1) and from the well head to the exact position of the pressure probe (d_2).

Step 3. “FFAWD Recovery test”:

- The valve is closed (Fig. 3a), which induces a rapid rise of the water level/pressure in the tube. The transformation of kinetic energy (water flowing up in the well tube at a significant velocity) into potential energy may cause some pressure fluctuations during the first few seconds after closure of the valve, as described further below. Then, the valve must not be closed too suddenly (closing duration: 2 to 3 s). The time at which the valve is closed must be noted. Nevertheless, it is also monitored by the pressure probe.
- A “recovery period” of about 30 min is recommended during which the pressure build-up (dP) is monitored with the sensor until pseudo-stabilization of H . The choice of the duration of this period is discussed in the following sections.
- Then the valve is re-opened and the finishing discharge (Q_{fin}) is measured (as well as the time of the measurements), similarly as in §3.c above.
- Then the device is removed, and the discharge (Q_0) is measured (as well as the time of the measurements), similarly as in Step 1.

Fig. 3b, shows a typical pressure graph obtained during this procedure.

Step 4. GPS measurements: a differential global positioning system (GPS), Trimble R6, was used to measure the precise coordinates (x, y, z) of the well head (or any other fixed landmark), based on the satellite signals received both at the rover and base stations (Parkinson and Spilker 1996). The geoid height is corrected considering the gradient of the local geoid (Kasenda et al. 2000). Then, the ellipsoid height measurements are converted into meters above sea level (m a.s.l.) using a digital elevation model (USGS SRTM30 dataset). With the differential GPS used here, the relative precision in z elevation between each well is about ± 10 cm.

Hydrodynamic response interpretation

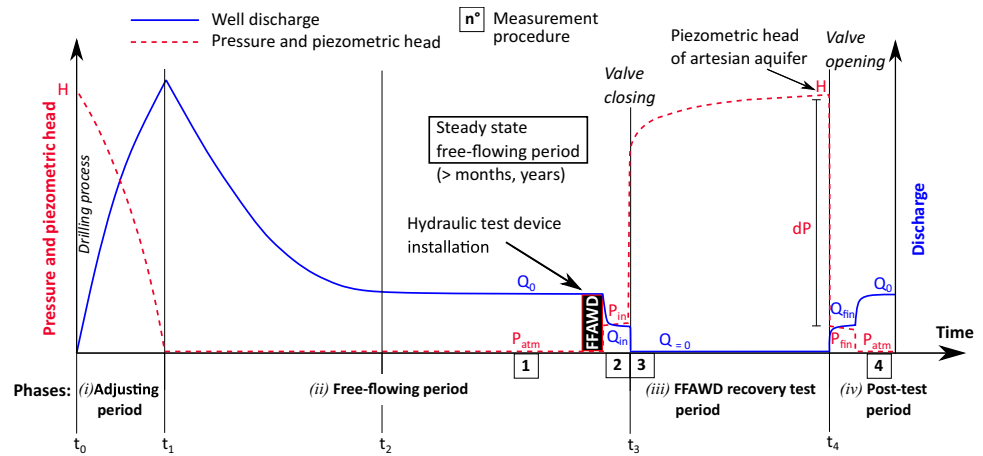
Description of the hydrodynamic response

Under such artesian conditions, the “FFAWD recovery test” is divided into four main phases, some of these phases being named by Sun and Xu 2014 (Fig. 4):

Phase (i), the “adjusting period” ($t_0 \rightarrow t_1$; Sun and Xu 2014), during which the well is drilled, with a discharge different from nil after the aquifer is reached. Once the top of the aquifer is drilled, the well discharge increases rapidly while the piezometric head is imposed to the well head elevation;

Phase (ii), the “free-flowing” period ($t_1 \rightarrow t_3$): this follows the rapid opening of the well that triggers a decrease in discharge. This period is the focus of most studies dealing with free-flowing wells (see for instance Sun and Xu 2014). In contrast to all those studies, the wells in this study were drilled several months or years before the test, without any well closure period, so the free-flowing period was long enough to reach a steady state. The discharge is considered as steady (as well as the one of nearby wells), and the piezometric head at the well is consequently also considered as stabilized, except during phase 2 of the device’s installation. This issue of steady state is addressed in the *Discussion* section of the paper; *Phase (iii)*, the “FFAWD recovery test period” ($t_3 \rightarrow t_4$): the closure of the well as described in section ‘*Design of the free-flowing artesian well device (FFAWD)*’ allows the pressure to increase inside the device, until it reaches equilibrium with the aquifer piezometric head. In the vicinity of the well, the piezometric head in the aquifer also increases;

Fig. 4 Schematic evolution of well discharge, piezometric head in the confined aquifer, and pressure measured with a probe installed at the top of the well head (or in our FFAWD). Modified after Sun and Xu (2014)



Phase (iv), the “Post-test period” ($t_4 \rightarrow t_\infty$): After reopening of the well and removal of the device, the well returns to its previous test conditions.

Each phase described above may enable computation of the aquifer hydrodynamic parameters through different interpretation methods, but the longer duration of two phases (the free-flowing and the FFAWD recovery test period) are considered to yield more robust results. The decrease of well discharge during the free-flowing period can be interpreted by a conventional method developed by Jacob and Lohman (1952), Hantush (1959) and Glover (1987). A simple approximation for the free-flowing well problem was provided by Swamee et al. (2002) using an error minimizing method to compute the discharge. Recently, the diagnostic plot method using the reciprocal rate derivative was adapted for the free-flowing test period by Sun et al. (2015). This phase is inappropriate in this study because the well discharge has been stabilized for a long time at the study site. Moreover, as discharge is generally measured with a lower precision than a piezometric head, this method is not very accurate, notably at the end of the test, when discharge variations decrease (see the *Discussion* section of the paper).

If the well is closed (again) after completion of a (short-duration) free-flowing period, the recovery test period (measurement of piezometric head) in transient state can be interpreted with the classical “Horner” recovery method in transient state (De Marsily 1986), taking into account notably the duration of the free-flowing period (see also Vuković and Soro 1992). This method does not fit with this case study, notably as the wells here are in steady state before the test, and thus cannot be applied. Thus, the focus is on the FFAWD test phase.

Computation of aquifer transmissivity

This study only surveyed “old” wells in steady free-flowing state (without any continuous discharge measurement since their drilling). The steady state discharge is then attained during this long free-flowing period. This steady state is stopped by the installation of the FFAWD. It allows use of the Houpeurt-Pouchan transient state recovery method (HPTSRM, De Marsily 1986). “Then, the recovery curve is interpreted as a drawdown curve with the help of either Jacob’s or Theis’s method” (De Marsily 1986) or any other appropriate analytical solution. In other words, the HPTSRM involves interpretation of the “recovery” observed after the installation of the FFAWD and the closure of its valve as a “classical” pumping test. The only difference is a negative discharge (Q_0 or Q_{in} , see Step 2 in section *Measurement procedure*) instead of a positive one, and a rising piezometric head instead of a decreasing piezometric head. To the authors’ best knowledge, nobody has described the use of this part of the evolution of the piezometric head for free-flowing wells, and the use of the HPTSRM.

Such a “recovery” test is usually not sensitive to well losses (Willmann et al. 2007) and can be easily interpreted with any appropriate analytical solution, as provided for instance by the software AQTESOLV (Duffield and Court 2007). The Cooper and Jacob (1946) method was already successfully used in other confined aquifers (Jacob 1940, 1947; Jacob and Lohman 1952; Wyrick and Floyd 1961; Merritt 1995) and was used in this research. This analytical solution considers the following simplifying assumptions: a single-well test assuming a confined, homogeneous, isotropic aquifer, with a vertical and fully penetrating well, taking into account the discharge rate (Q) and the distance from the

well (r). The Cooper-Jacob logarithmic approximation of the Theis solution is given by:

$$s = \frac{Q}{4\pi T} \ln \frac{2.25Tt}{Sr^2} \quad (3)$$

where:

- s drawdown at the (observation) well (= well and recovery curve in this case) (m)
- Q discharge (here, before closing the valve) ($\text{m}^3 \text{s}^{-1}$)
- T transmissivity ($\text{m}^2 \text{s}^{-1}$)
- t time since the start of pumping (= time since the beginning of the FFAWD recovery test period) (s)
- S storage coefficient (-)
- r the distance between the well and the observation well (piezometer), or the radius of the well in case of the observation is performed at the well itself.

Whence

$$T = \frac{2.3}{4\pi} \cdot \frac{Q}{\Delta s} \quad (4)$$

and

$$S = \frac{2.25Tt_0}{r^2} \quad (5)$$

where:

- Δs : drawdown measured during one log cycle
- t_0 : the time at which the Jacob straight line intersects the $s = 0$ line

Equation (4) is solved graphically with AQTESOLV on a semi-logarithmic grid by plotting values for the ratio of drawdown on the linear (Y) scale against corresponding values of time (t) on the logarithmic (X) scale. Then, the T value is calculated using the Cooper-Jacob matching-curve method (Jacob straight-line) and considering a constant derivative period of 1 log-cycle of t (Δs) (Renard 2005). Note that in this case it was not possible to calculate the storage coefficient (S) (Eq. 5), as the test is performed without a piezometer. This concern will be discussed in detail in the *Discussion* section. More complex analytical solutions than the Cooper-Jacob one can be used to interpret the test, if required considering the shape of the observed curves. It will be seen in the *Results* section that this was not necessary with the data set used here.

Computation of well-bore storage effect

To avoid any artefacts, it is first necessary to distinguish the well-bore storage effect, called the “post-production effect” (Ungemach et al. 1968; Forkasiewicz 1972) which occurs during the early stage of the FFAWD test, after the discharge of the well has stopped. During that period, it is impossible to estimate the transmissivity of the aquifer. For each well, information given by the derivative curve from Bourdet et al. (1989) is compared with a numerical estimation provided by Eq. (6) (Forkasiewicz 1972), that computes the duration of the “post-production effect”:

$$t = \frac{25r_d^2}{T} \quad (6)$$

where:

- t duration of the post-production effect (s)
- r_d radius of the tube constituting the FFAWD (m)
- T transmissivity ($\text{m}^2 \text{s}^{-1}$)

Then, FFAWD recovery tests were interpreted for 16 free-flowing artesian wells.

Piezometric and Transmissivity mapping

The piezometric head H of the confined aquifer at the measured free-flowing well is obtained at the end of the “FFAWD recovery test period” (Fig. 4). In addition, other piezometric heads from manual measurements performed on flowing artesian springs, a lake and non-flowing artesian wells were also used to complete the dataset, as well as FFAW where the device was used, but without monitoring the head rise and thus computing T (see Table 1 and the electronic supplementary material (ESM)). The representativity of these different values of H will be discussed in the *Discussion* section.

Case study

The free-flowing artesian well device (FFAWD) was applied in the artesian plain of Pasuruan covering about 200 km², located in the north of the Bromo-Tengger volcano in East Java, Indonesia. A detailed description of the geology and the aquifer conceptual model is provided by Toulhier et al. (2019) and in the ESM.

Among all the free-flowing wells inventoried, 28 were selected (applying the criteria described in section *Measurement procedure*) for applying the device and developing

Table 1 Characteristics of artesian water points and results obtained. The piezometric data refer to four types: artesian springs (AS), non-flowing artesian wells (NFAW), free-flowing artesian wells (FFAW) and surface water (LAKE). Transmissivity (T) is computed only at the FFAWs except those where the FFAWD was installed but where the test period was not monitored. For unmonitored FFAWDs, the piezometric head was only measured visually on the device at the end of the test

Water point description		FFAWD recovery test results										Piezometric head results			
Well No.	Type	X (m)	Y (m)	Depth below ground surface (m b.g.s)	Ground elevation from GPS (m a.s.l.)	Casing diam. out (mm)	Flow Q_{in} ($L s^{-1}$)	FFAWD test duration ($t_3 \rightarrow t_4$) (s)	Water level above ground surface (at t_4) (m a.g.s.)	T ($m^2 s^{-1}$)	Post production effect duration (s)		Observed effects (Fig. 5)	Piezometric level (at t_4) (m a.s.l.)	Reliability (see ESM)
											Computed	Measured			
		(UTM49S)													
1	Umbulan	AS	713304	9141736	-	31.95	-	3500.0	-	Surface water	-	-	-	32.10	H1
2	Banyu Biru	AS	717072	9143018	-	29.43	-	350.0	-	Surface water	-	-	-	28.47	H1
3	FD2	FFAW	717239	9142550	32	37.36	904	0.2	2999	0.99	3.10×10^{-3}	23.4	40	Fig 5a	H1
4	Truck	FFAW	717107	9144385	50	19.86	1146	8.0	-	> 2.85	-	-	-	22.71	H2
5	AWQ	FFAW	716558	9142195	60	39.83	904	0.9	2093	0.74	8.83×10^{-3}	8.4	20	Fig 5b	H1
6	FD1	FFAW	715390	9142385	103	38.22	904	1.9	1903	3.72	1.06×10^{-3}	69.5	50	Fig 5b	H1
7	Pasir Well	FFAW	715907	9143728	40	19.61	1146	8.6	< 300	3.14	-	-	-	22.75	H2
8	BenbyAlix	FFAW	716175	9144539	63	17.18	773	4.8	1973	2.46	3.45×10^{-3}	21.4	25	Fig 5b	H1
9	BanyuCam	FFAW	716969	9143232	66	29.32	1146	6.0	< 60	3.56	-	-	-	32.88	H2
10	F8	FFAW	715723	9145698	40	15.86	904	10.0	< 60	7.47	-	-	-	23.33	H2
11	Aqua Wash	FFAW	714339	9146170	96	16.54	1400	15.0	-	> 5.2	-	-	-	21.74	H2
12	AW6	FFAW	720216	9146694	120	16.02	621	0.1	1924	1.85	4.01×10^{-4}	183.8	190	Fig 5a	H1
13	Aqua Piezo	FFAW	713213	9145881	70	19.61	904	12.7	25397	3.48	1.11×10^{-2}	6.6	20	Fig 5b	H1
14	AW24	FFAW	713888	9144172	60	22.52	904	4.8	< 300	3.98	-	-	-	26.50	H2
15	AW2	FFAW	709387	9149073	93	24.61	1146	6.0	2097	6.02	2.64×10^{-3}	27.9	30	Fig 5a	H1
16	P13	NFAW	722866	9145631	30	28.95	1146	-	-	-2.54	-	-	-	26.41	H1
17	Ranu Grati	LAKE	721382	9145180	120	23.30	-	-	-	Surface water	-	-	-	22.88	H1
18	Michel	FFAW	714150	9144515	38	22.36	904	6.0	1420	3.68	2.91×10^{-2}	2.5	150	Fig 5c	H2
19	AW27	FFAW	711747	9143939	60	32.63	904	4.3	1878	5.77	2.36×10^{-3}	31.3	50	Fig 5a	H1
20	AW15	FFAW	712173	9142980	52	37.72	1146	6.7	679	2.86	1.00×10^{-2}	7.4	10	Fig 5c	H2
21	B33	FFAW	710227	9143490	88	44.90	1146	2.1	610	1.13	4.05×10^{-2}	1.8	15	Fig 5b	H1
22	West Umb	FFAW	710267	9143352	133	44.29	1146	18.2	2129	5.08	4.32×10^{-2}	1.7	15	Fig 5c	H2
23	AW16	NFAW	708369	9143299	140	66.20	1146	-	-	-6.74	-	-	-	59.46	H1
24	AW21	FFAW	708963	9145059	129	46.60	1146	3.2	1800	0.96	-	-	-	47.56	H2
25	AW74	FFAW	709306	9145872	79	36.26	1146	3.1	1935	3.03	2.04×10^{-3}	36.1	30	Fig 5c	H2
26	AW23	FFAW	711390	9145489	83	31.61	1146	5.2	1069	6.12	2.14×10^{-3}	34.4	30	Fig 5a	H1
27	AW14	FFAW	711972	9147092	60	22.16	1146	8.0	225	2.12	2.62×10^{-2}	2.8	20	Fig 5b	H1
28	B23	FFAW	707564	9147142	81	36.96	1146	11.2	2097	5.5	5.24×10^{-3}	14.1	30	Fig 5b	H1
29	B19	FFAW	707594	9146821	150	37.88	904	35.0	< 60	7.26	-	-	-	45.14	H2
30	AW33	FFAW	705998	9146529	200	44.48	904	12.7	< 60	7.69	-	-	-	52.17	H2

Table 1 (continued)

Well No.	Water point description				FFAWD recovery test results						Piezometric head results				
	Name	Type	X (m)	Y (m)	Depth below ground surface (m b.g.s)	Ground elevation from GPS (m a.s.l.)	Casing diam. out (mm)	Flow Q_{in} ($L\ s^{-1}$)	FFAWD test duration ($t_3 \rightarrow t_4$) (s)	Water level above ground surface (at t_4) (m a.g.s.)	T ($m^2\ s^{-1}$)	Post production effect duration (s)		Piezometric level (at t_4) (m a.s.l.)	Reliability (see ESM) (Fig. 5)
												Computed	Measured		
31	Pylone	FFAW	711954	9148334	100	17,08	1146	10.0	-	> 5.15	-	-	-	22.23	H1: Good H2: Medium
32	Grogol 1	FFAW	712270	9149088	60	15,07	1146	12.0	< 60	> 8.8	-	-	-	23.87	H2
33	Grogol 2	FFAW	712021	9149008	60	16,25	1146	15.5	< 60	> 8.5	-	-	-	24.75	H2

the methodology presented. That includes 16 FFAWD test interpretations, enabling one to compute the transmissivity and measure the piezometric head, and 12 FFAWD tests enabling only measurement of the piezometric head (the piezometric rise was not monitored). In addition, two non-flowing artesian wells, as well as two artesian springs and one lake supplied by the confined aquifer, were also considered for the piezometric mapping.

All the measurements were performed over a short period of time, from May to June 2018, to obtain a synchronous piezometric map. Table 1 reports the characteristics of the wells, springs and lake, along with the results obtained.

Results

Computation of hydrodynamic parameters

The FFAWD recovery test parameters for the 16 free-flowing wells are reported in Table 1. The semi-log curves (Fig. 5) show a post-production effect followed by a period of piezometric head rise corresponding to the aquifer response. Overall, three types of curves can be distinguished:

- a. *Ideal FFAWD test with post-production* (Fig. 5a): the entire test does not seem to be disturbed by any external effects (except post-production). The inflection point of the drawdown curve after the post-production effect is followed by a second phase of constant rise over time (confined aquifer without any limit or leak) which enables computation of T . The slope of the line is steady after the end of post-production. The end of the post-production effect corresponds to the end of the hump in the derivative curve. It is visually delimited by the vertical black dotted line on Fig. 5.
- b. *FFAWD test with surge* (Fig. 5b): the beginning of the FFAWD test is impacted by a water hammer effect due to the too fast closure of the well, which causes a sudden change in water velocity in the well (down to zero). The corresponding kinetic energy is converted into piezometric head (Vasquez 2010) and triggers sinusoidal fluctuations. This can mask the inflection point of the curve at the end of the post-production phase (and thus partly hide the post-production) but does not affect the part of the curve for which interpretation is critical to compute the transmissivity (Wyrrick and Floyd 1961). As the authors experienced such surges during the tests, it is recommended in Step 3 in section *Measurement procedure* to close the valve slowly, particularly in wells with a high discharge (relative to well diameter).
- c. *FFAWD test with leaks* (Fig. 5c): the inflection point of the post-production phase remains clearly visible. After

a first phase of constant recovery, recovery is influenced by leaks in the well or, less probably, from the aquifer itself (leakage). This leak effect reduces the slope of the curve, or even the piezometric head, at wells. The leakage increasing with time is interpreted by the de-clogging of the well annulus. The unaffected part of the curve (here on Fig. 5c between 10 and 100 s) should be used to compute the aquifer transmissivity. In the case of a leaky aquifer, the affected part of the curve can be interpreted with an appropriate analytical solution to characterize aquifer leakage parameters.

Some FFAWD recovery curves can combine the three types effects presented here (surge, post-production, and leaks), even though the post-production effect is often masked when there is a surge.

A compilation of the FFAWD test results shows that:

- The post-production duration ranges from a few seconds to 180 s depending on the well (30 s on average). A comparison of the durations of the post-production effect, computed from Eq. 6. and graphically determined, shows no significant discrepancies. Only well n°18 shows an inconsistent result but the transmissivity value used in Eq. 6 is probably overestimated as suggested by the leak effect (type c) considered for this well (Fig. 6a). Thus, globally, this post production effect is well understood and computed. The intercept or the regression curve (about 10 s) means that the observed post-production effects are about 10 seconds longer than the computed

ones. This is surely due to an additional volume of the FFAWD that is larger in the section with the valve (Fig. 3) than elsewhere (tube only); in fact, the diameter of the tube was used to compute the theoretical duration of the post-production effect, and the section with the valve was not considered.

- The constant log-log derivative curves at long duration (e.g. between 80 to 1000 s in Fig. 5a) confirm that the response of the aquifer well follows the Cooper-Jacob straight line. A two-dimensional infinite acting radial flow model (IARF) can be assumed, describing a flow converging towards the circular cylinder of the well (Renard et al. 2009). Thus, no more complex analytical solution (for instance with well partial penetration effect) is required in this case study. The transmissivity results range from 10^{-2} to 10^{-4} $\text{m}^2 \text{s}^{-1}$, with an arithmetic average value of 10^{-3} $\text{m}^2 \text{s}^{-1}$.

Results for the Pasuruan artesian plain, Indonesia

The results of the FFAWD application including the piezometric and transmissivity maps are provided in the ESM.

Discussion

The FFAW device

The device developed in the framework of this research (FFAWD) shows the following advantages:

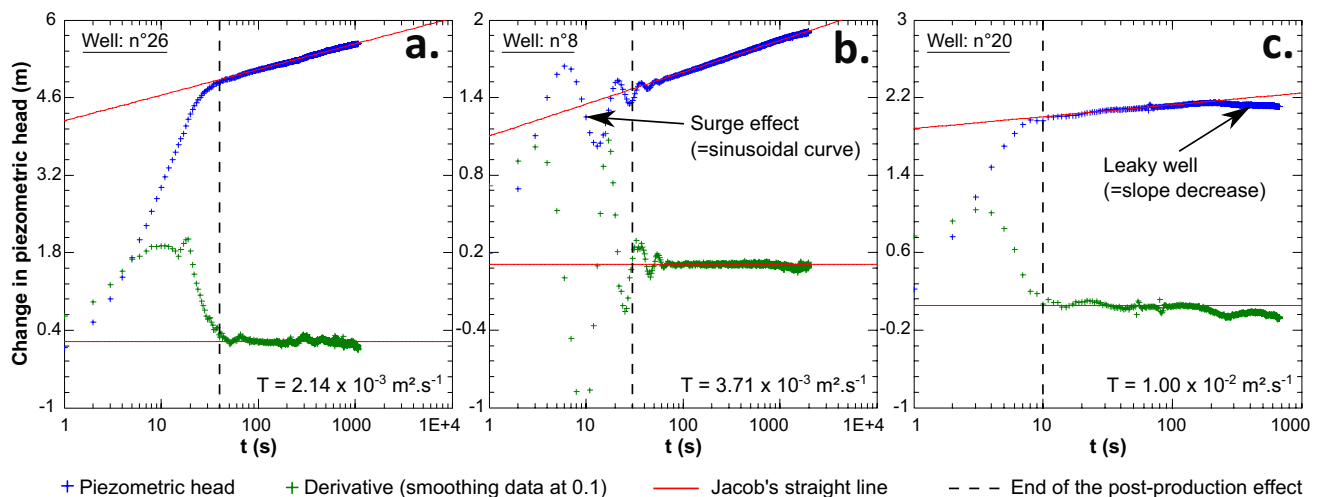


Fig. 5 Representative piezometric head data recorded during the FFAWD tests at wells, sorted into three categories: **a.** well n°26: recovery curve without any visible influence, except for post-production effects, **b.** well n°8: recovery curve influenced by surge effect during the first tens of seconds of the test (=sinusoidal curve), the

post-production is largely masked, and **c.** well n°20: recovery curve influenced by leaky well or internal leakage within the aquifer itself (in addition with post-production effect). All the FFAWD recovery test periods are interpreted with the Cooper-Jacob solution (red curves)

- It is easy to build (PVC pipe and valve available everywhere in the world) and low cost: less than 100€, pressure sensor not included;
- It is very fast (<10 min) to install on various diameter/discharge wells and easy to deploy in the field by 2 operators. It is much less convenient if the operator is alone, which must be avoided;
- No external power supply is required;
- The visibility of the water within the transparent pipe during measurements is important, notably to see and visually follow the evolution of the water level during its early phase, and to visually check the progress of the test. This also reassures the local population/owner of the well that the water is “still there”, even if the well ceases to flow during the test;
- The obtained data are accurate and reliable.

The following shortcomings of the device could be resolved in the future:

- Beyond 8 m of piezometric head above ground surface, the tubes (4 x 2 m) become unstable and a supplementary shoring system is necessary. A lightweight telescopic scaffolding as used in civil engineering could effectively stabilize the tubes. The diameter of the tubes could also be reduced to decrease the weight of the FFAWD during its operation, but with strong enough tubes to maintain the required rigidity of the device;
- The use of other probes (e.g., CTD Diver) may provide monitoring of additional physico-chemical parameters during the hydraulic test (EC, temperature, pH, etc.). It might enable one to detect well leakage (Fig. 5c).

Method of measurement

First, the method using several PVC pipes (keeping a free water surface) was preferred to the method involving the

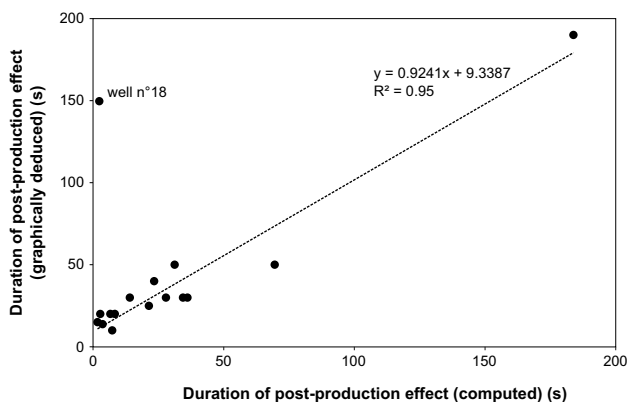


Fig. 6 Comparison of the duration of the post-production effect between computed values (Eq. 6 from Forkasiewicz (1972)) and values graphically determined from the derivative curve

closure of the artesian well. From the authors’ experience, the water pressure makes it very difficult to completely close the well. For instance, the free-flowing artesian well device (FFAWD) developed here is hard to maintain in place under such a high-pressure head (> 6 m) and would require an additional fixing system.

Even with the FFAWD, if the well grouting is not totally impervious (no grouting or casing/grouting too short and/or in poor condition), a leak between the well casing and the rock may appear during the test as diagnosed for wells n° 18, 20, 22 and 25 (Table 1; observed leakage effect as shown in Fig. 5c). Another type of leak may occur inside the aquifer itself, especially in open-hole wells where two water-bearing formations have different piezometric heads, such as in a multi-layered system classically found in volcano-sedimentary plains (Selles et al. 2015). Thus, the selection of free-flowing artesian wells with a good visual aspect is a priority before applying the device on large scale, even if it is not a guarantee of no leaks. A concrete base around the well head is a good indication that the well is probably less liable to leak, although this is not always the case. Nevertheless, most observations with leakage at the well enabled one to compute T .

As regards the duration of measurements, a recovery period of 30 min is appropriate because (i) it does not cut off water access to the local population for an excessive period (e.g. paddy field irrigation or domestic use); and (ii) most of the tested artesian wells with different configurations (transmissivity, discharge, depth, etc.) provided a well-defined Jacob’s straight line on the drawdown curve, allowing one to easily compute T .

Data interpretation

The interpretation of FFAWD recovery tests by the Cooper-Jacob method yields consistent transmissivity results in this case study, ranging over 1 to 2 orders of magnitude (from 10^{-2} to 10^{-4} $\text{m}^2 \text{s}^{-1}$). Transmissivity is probably overestimated for at least well n°18 which is influenced by leaks, with values of about 10^{-2} $\text{m}^2 \text{s}^{-1}$; but the analysis of the Bourdet derivative allows one to avoid possible bias related to (1) post-production effects (\approx well-bore storage) and (2) leaks related to the well casing or the aquifer itself, by applying the Cooper-Jacob straight line on a constant derivative period. Thus, there is finally no real issue with such leaks. In this case study, the simple Cooper-Jacob solution is appropriate to interpret the data. However, other more complex analytical solutions could be used if necessary to account for anisotropy and incomplete well effects, a discussion of which is beyond the scope of this paper.

The discharge Q_{in} was used to calculate the transmissivity; it corresponds to the discharge measured before closing

the valve of the device. Theoretically, it would have been better to use Q_0 , measured before installing the FFAWD on the well head. However, the precision on Q_0 is usually lower than the one on Q_{in} as discharge measurements are often hard to perform on a well head that protrudes little above the ground. Using Q_{in} instead of Q_0 does not significantly influence the transmissivity computation. Measurements show that the discharge Q_{in} is about 3 to 5% lower than Q_0 (depending on the length of the PVC connections installed); then, the computed transmissivity is about 3 to 5% lower than the actual one, and can easily be corrected with Q_0 measurements, although there is much lower accuracy than the Q_{in} measurements. Experience gained during this research shows that the stabilization to Q_{in} is very fast (not measurable in fact, the repeated Q_{in} measures being within the uncertainty range of the stabilized Q_{in} value).

FFAW tests are performed in such an aquifer where, due to the year after year abstraction increase, the piezometric level is declining with time and the discharge of each wells is also declining. Thus, two FFAW tests performed at two dates separated by several years will have the following characteristics:

- The first test will exhibit a higher discharge than the second one, but also, consequently, a higher slope of the Cooper-Jacob straight line (Eq. 4);
- The second test will exhibit a lower discharge but also a lower slope of the Cooper-Jacob straight line.

Consequently, the computed transmissivity will be the same whatever the date of the completion of the FFAW test. In fact, as for any pumping test, there is no bias related to the discharge of the well during the pumping test. The computed transmissivity is the same whatever the discharge of the pumping test.

In this case study, the piezometric head measured at the end of the FFAWD test period (good reliability (H1) and medium reliability (H2) in Table 1), that rarely exceeded 30 min, was used to draw a piezometric map. However, not all recovery tests performed during this field campaign had the same duration. Moreover, the recovery was not totally completed during most tests, and the recovery rate is also well-dependent, as not all free-flowing wells have the same discharge; well discharge depends notably on the local hydrodynamic conditions (T and S) and piezometric head. A sensitivity analysis to estimate these impacts on the computed piezometric head was thus performed and showed that the homogenization of the data may require a piezometric correction ranging, for this case study, between -0.70 and $+0.79$ m, but with 75% of the wells having corrections ranging only between -0.2 and $+0.2$ m. It then appears that, for this case study and the chosen application (basin-scale piezometric mapping for which about 1 m accuracy is enough),

such a correction is not necessary. The conclusion would not be identical for a high-resolution piezometric mapping, at the scale of a civil engineering project for instance, requiring piezometric levels with a centimeter accuracy. The sensitivity analysis computation was performed at each well, based on the estimation of the time required to recover, with the transient-state Jacob analytical solution (De Marsily 1986), and the steady state drawdown at the well computed with the Dupuit analytical solution (De Marsily 1986), considering a complete recovery minus 1 m. For calculation, this study used a confined aquifer with a 10^{-4} storage coefficient, the transmissivity computed at the well and a geometry (distance to aquifer limits notably) similar to the one of the studied Pasuruan aquifer (less than 10 km).

Similar computations with the same parameters were performed to check that all FFAWs can be considered in steady state before completion of the tests. They show that such a steady state is obtained in a few months after the drilling of the FFAW (2 to 3 months). As most studied FFAW were drilled years ago, this assumption is valid.

Computing the aquifer storage coefficient

From aquifer tests, it is well known (see for instance Kruseman and Ridder 1971; De Marsily 1986) that the storage coefficient cannot be computed from data obtained at the pumping well as there is a large uncertainty on the well effective diameter, and also as well clogging or overdevelopment quite often shifts the drawdown curve. Such a shift, theoretically, has no influence on the computation of T (notably if the discharge is steady), or it can be overcome. However, it strongly influences the location of the intersect of the Jacob straight line with the zero-drawdown line. Thus, an observation well (piezometer) is mandatory for that purpose, which wasn't the case in the research report here. Additionally, for classical pumping tests, S cannot be obtained from the recovery data (residual drawdown) obtained after the completion of a pumping with the Theis or the Cooper-Jacob methods (Todd and Mays 2005). Some authors, nevertheless developed new methods to compute the storage coefficient from single-step pumping test recovery data (Banton and Bangoy 1996; Ashjari 2013), from multi-step pumping test recovery data (Lee and Lee 2000) or from the Agarwal recovery test method (Trabucchi et al. 2018). However, all these methods require data from a piezometer. For free-flowing wells, some authors proposed to compute the storage coefficient based on single-well tests, by monitoring the drawdown and the discharge at the well after opening it (Jacob and Lohman 1952; Ojha 2004; Wendland 2008; Perina 2021) (i.e. the well is opened after a long period without flow). These authors claim that no piezometer is required since they assume the well to have an infinitesimal radius (i.e.

the “effective radius” of the well is used by Jacob and Lohman 1952). In the case reported here, no continuous discharge measurement was performed (nevertheless, instead, piezometric levels were observed, which is equivalent), no piezometer was available near the tested free-flowing wells, and the effective radius of the wells was unknown. Nevertheless, the storage coefficient was computed with the Cooper-Jacob method (Kruseman and Ridder 2000) and the real radius of the well (radius of tube). It resulted in physically unacceptable values: 13 values between $S = 3.10^{-83}$ and 3.10^{-9} , and only three “more acceptable” values: 1.10^{-4} , 3.10^{-6} , and 9.10^{-6} . This demonstrates, if any proof were needed, that S can hardly be computed from data observed at the well. Moreover, the very low values of the computed S suggest very small effective radius, and thus that most the wells in the study area are clogged (rather than overdeveloped).

As a solution to compute S , it would be worthwhile to build several FFAWDs. They could then be installed on nearby FFAWs to not only compute T and H at these different wells, but also to trigger interferences between them and thus enable the computation of the storage coefficient S from the aquifer. A simple procedure is then:

1. The FFAWDs would be installed, and their valve closed on FFAWs surrounding the studied FFAW.
2. Then, after H reaches an equilibrium at all these wells (this transient period being monitored to compute T and H), sequences of closing and opening the valve at the studied FFAW would be performed. This FFAW and the surrounding ones (with closed valves) would be monitored.
3. These tests would be interpreted as for any pumping test performed with piezometers in an aquifer.

A first sensitivity analysis shows that such a S computation should be feasible in such a confined aquifer where the drawdown propagates fast and far. Computations were performed with the Cooper-Jacob analytical solution with $T = 1.10^{-3} \text{ m}^2 \text{ s}^{-1}$, $S = 1.10^{-4}$, and a tested FFAW with a 5 L s^{-1} discharge. They show that interferences of about 30 cm are obtained at a distance of 200 m one hour after the valve is closed (or reopened). The interferences are about 80 cm at a 100 m distance, far enough to compute T and S from these data. The interferences are already 55 cm after half an hour at 100 m, but only a few millimeters at 200 m. Practically, on the Pasuruan aquifer, the tests applied on “piezometers” equipped with a FFAWD could be performed in a 100–150 m radius around the tested FFAW. This appears highly feasible considering the density of FFAWs in that area. In any other aquifer, the feasibility could be assessed a priori with such a rough computation.

Case study: insights on the aquifer’s functioning

Based on the case study provided in the ESM, the transmissivities (from 10^{-2} to $10^{-4} \text{ m}^2 \text{ s}^{-1}$) are relatively high and very consistent with other volcanic contexts (Hunt 1996; Singhal and Gupta 2010; Charlier et al. 2011; Lachassagne et al. 2014; Selles 2014; Dumont et al. 2021). The groundwater flows northward from the northern flank of the volcano to the volcano-sedimentary aquifer of Pasuruan. The piezometric pattern indicates a recharge zone from the volcano and a discharge zone spreading in the plain through the free-flowing artesian wells and artesian springs’ outflows. The hydraulic gradients range from 0.001 to 0.01.

A periodic deployment of the FFAWD for piezometric surveys of the Pasuruan artesian basin could provide robust information about the evolution of the piezometry and be used as a decision support tool for water resources stakeholders.

Conclusion

The design of a low-cost field-built device that is easy to reproduce and adaptable to various conditions, the free-flowing artesian well device (FFAWD), is described in this paper, as well as the method to set it up in the field, in aquifers where free-flowing wells are not valved and have been continuously flowing for months or years.

The principle of the method is (i) to install the FFAWD on the well head, its valve open, allowing to (ii) measure the discharge of the free-flowing well; then, (iii) to close the valve that allows the pressure to increase inside the FFAWD, and be monitored with a sensor. At the end of the test, (iv) the valve is open again; (v) the discharge is measured once more, and the FFAWD is uninstalled.

The obtained data set is the discharge of the free-flowing well, and pressure increase measurements after its valving with the FFAWD. The test is interpreted as a single-well pumping test. A method is proposed to compute the piezometric head and the transmissivity of the aquifer from this data set, using the Houpeurt-Pouchan method and any adapted analytical solution (such as the Cooper-Jacob analytical solution). Artefacts, such as post-production, surge effect, and impact of a leaky well, are identified and described to avoid any misinterpretation.

The FFAWD was successfully applied on the volcano-sedimentary artesian plain of the Bromo-Tengger volcano (Indonesia) for transmissivity and piezometric mapping.

The advantages and limitations of the device and method are discussed, as well as perspectives such as the way to homogenise H data sets with various durations of the recovery period or various T and piezometric heads, and the way to compute the storage coefficient of the aquifer. It also

demonstrates the kind of simple but accurate instrument that can be built from local store-bought items when budgetary limitations prohibit the purchases of more sophisticated equipment.

The roll out of this device can help in improving the conceptual model of other artesian basins worldwide. It can also provide useful data to set up a numerical model for water resources management, to support implementation of solutions to guarantee the long-term groundwater resource sustainability.

Supplementary Information The online version contains supplementary material available at <https://doi.org/10.1007/s10040-022-02505-5>.

Acknowledgements This research was carried out as part of a PhD thesis in the framework of the Rejoso Kita project, which is co-directed by Danone AQUA, the International Centre for Research in Agroforestry (ICRAF), the Social Investment of Indonesia (SII) and the CKNet foundation, with the financial support of Danone Indonesia. Scientific and logistic support from Gadjah Mada University is gratefully acknowledged. The authors gratefully acknowledge the partnership and authorizations provided by the Ministry of Research, Technology and Higher Education of Indonesia (RISTEKDIKTI) and the Bromo Tengger Semeru National Park (TNBTS). Dr M.S.N. Carpenter post-edited the English style and grammar in an early version. The executive editor Cliff Voss, the editor J.C. Comte and the two anonymous reviewers are also warmly thanked for their careful reviews which helped to improve the manuscript

Declarations

Conflict of interest On behalf of all authors, the corresponding author states that there is no conflict of interest.

Open Access This article is licensed under a Creative Commons Attribution 4.0 International License, which permits use, sharing, adaptation, distribution and reproduction in any medium or format, as long as you give appropriate credit to the original author(s) and the source, provide a link to the Creative Commons licence, and indicate if changes were made. The images or other third party material in this article are included in the article's Creative Commons licence, unless indicated otherwise in a credit line to the material. If material is not included in the article's Creative Commons licence and your intended use is not permitted by statutory regulation or exceeds the permitted use, you will need to obtain permission directly from the copyright holder. To view a copy of this licence, visit <http://creativecommons.org/licenses/by/4.0/>.

References

- Ashjari J (2013) Determination of storage coefficients during pumping and recovery. *Groundwater* 51:122–127. <https://doi.org/10.1111/j.1745-6584.2012.00917.x>
- Banton O, Bangoy L (1996) A new method to determine storage coefficient from pumping test recovery data. *Groundwater* 34:772–777. <https://doi.org/10.1111/j.1745-6584.1996.tb02069.x>
- Banton O, Bangoy LM (1997) Hydrogeologie. Multiscience environnementale des eaux souterraines [Hydrogeology. Environmental multiscience of groundwater]. Presses de l'Université du Québec/AUPELF
- Bourdet D, Ayoub JA, Pirard YM (1989) Use of pressure derivative in well test interpretation. *SPE Form Eval* 4:293–302. <https://doi.org/10.2118/12777-pa>
- Charlier JB, Lachassagne P, Ladouche B, Cattan P, Moussa R, Voltz M (2011) Structure and hydrogeological functioning of an insular tropical humid andesitic volcanic watershed: A multi-disciplinary experimental approach. *J Hydrol* 398:155–170. <https://doi.org/10.1016/j.jhydrol.2010.10.006>
- Chen J, Wilson CR, Famiglietti JS, Scanlon BR (2018) 4.12 - Groundwater storage monitoring from space. In: Liang S (ed) *Comprehensive Remote Sensing*. Elsevier, Oxford, pp 295–314
- Cooper HH, Jacob CE (1946) A generalized graphical method of evaluating formation constants and summarizing well-field history. *Trans Am Geophys Union*;14
- De Marsily G (1986) Quantitative hydrogeology. Groundwater hydrology for engineers. Academic press
- Duffield GM, Court H (2007) AQTESOLV for windows version 4.5 user's guide
- Dumont M, Reninger PA, Aunay B, Pryet A, Jougnot D, Join JL, Michon L, Martelet G (2021) Hydrogeophysical characterization in a volcanic context from local to regional scales combining airborne electromagnetism and magnetism. *Geophys Res Lett* 48:1–11. <https://doi.org/10.1029/2020GL092000>
- Flook S, Fawcett J, Cox R, Pandey S, Schöning G, Khor J, Singh D, Suckow A, Raiber M (2020) A multidisciplinary approach to the hydrological conceptualisation of springs in the Surat Basin of the Great Artesian Basin (Australia). *Hydrogeol J* 28:219–236. <https://doi.org/10.1007/s10040-019-02099-5>
- Forkasiewicz J (1972) Interprétation des données de pompages d'essai pour l'évaluation des paramètres aquifères. Aide-Mémoire [Interpretation of pumping tests data for the determination of aquifer parameters. Aide-mémoire]
- Freeze RA, Cherry JA (1979) *Groundwater*. Prentice-Hall. Inc., Englewood Cliffs
- Glover RE (1987) *Transient groundwater hydraulics*. Water Resource Publications, LLC, Colorado
- Habermehl MA (2020) Review: The evolving understanding of the Great Artesian Basin (Australia), from discovery to current hydrogeological interpretations. *Hydrogeol J* 28:13–36. <https://doi.org/10.1007/s10040-019-02036-6>
- Hantush MS (1959) Nonsteady flow to flowing wells in leaky aquifers. *J Geophys Res* 64:1043–1052. <https://doi.org/10.1029/jz064i008p01043>
- Hunt CD (1996) *Geohydrology of the Island of Oahu, Hawaii*
- Jacob CE (1940) On the flow of water in an elastic artesian aquifer. *EOS Trans Am Geophys Union* 21:574–586. <https://doi.org/10.1029/TR021i002p00574>
- Jacob CE (1947) Radial flow in a leaky artesian aquifer. *EOS Trans Am Geophys Union* 28:481–484. <https://doi.org/10.1029/TR028i003p00481>
- Jacob CE, Lohman SW (1952) Nonsteady Flow to a Well Of Constant Drawdown. *Am Geophys Union* 33:10
- Jiang XW, Wan L, Wang XS, Wang D, Wang H, Wang JZ, Zhang H, Zhang ZY, Zhao KY (2018) A multi-method study of regional groundwater circulation in the Ordos Plateau, NW China. *Hydrogeol J* 26:1657–1668. <https://doi.org/10.1007/s10040-018-1731-4>
- Jiang XW, Cherry J, Wan L (2020) Flowing wells: Terminology, history and role in the evolution of groundwater science. *Hydrol Earth Syst Sci* 24:6001–6019. <https://doi.org/10.5194/hess-24-6001-2020>
- Kasenda A, Komara AM, Sutisna S (2000) The Indonesian gravity field and the geoid model. In: Rummel R, Drewes H, Bosch W, Hornik H (eds) *Towards an Integrated Global Geodetic Observing System (IGGOS)*. Springer, Berlin Heidelberg, pp 245–247

- Khasanah N, Tanika L, Pratama LDY, Leimona B, Prasetyo E, Marulani F, Hendriatna A, Zulkarnain MT, Toulrier A, van Noordwijk M (2021) Groundwater-extracting rice production in the Rejoso watershed (Indonesia) reducing urban water availability: characterisation and intervention priorities. *Land* 10. <https://doi.org/10.3390/land10060586>
- Kruseman GP, Ridder NA (2000) Analysis and evaluation of pumping test data, 2nd editio
- Lachassagne P, Aunay B, Frissant N, Guilbert M, Malard A (2014) High-resolution conceptual hydrogeological model of complex basaltic volcanic islands: A Mayotte, Comoros, case study. *Terra Nov* 26:307–321. <https://doi.org/10.1111/ter.12102>
- Lee J-Y, Lee K-K (2000) A general solution of determining storage coefficient from multi-step pumping test recovery data. *J Korean Soc Groundw Environ* 7:22–23
- Legette R, Taylor G (1934) The transmission of pressure in artesian aquifers. *US Geol Surv Prof Pap*:409–413
- Lin L (2007) Hydraulic properties of the Table Mountain Group (TMG) aquifers. Faculty of Natural Sciences, University of the Western Cape
- Lohman SW (1965) Geology and artesian water supply, Grand Junction area. *Colorado Geol Surv water-supply Pap* 451:149
- Margat J, Pennequin D, Roux J-C (2013) Histoire de l'hydrogéologie française [History of french hydrogeology]. Orléans
- Meinzer OE (1928) Compressibility and elasticity of artesian aquifers. *Econ Geol* 23:263–291. <https://doi.org/10.2113/gsecongeo.23.3.263>
- Meinzer OE, Hard HA (1925) Contributions to the hydrogeology of the unites states. *Geol Surv water-supply Pap*
- Merritt ML (1995) Computation of the time-varying flow rate from an artesian well in central Dade County, Florida, by analytical and numerical simulation methods
- Nichols WD, Shade PJ, Hunt Jr. CD (1996) Summary of the Oahu, Hawaii, regional aquifer-system analysis
- Oberlander PL, Almy RB (1979) Aquifer tests report for stage Gulch Ranch well no 3, Standfield, Oregon. Standfield
- Ojha CSP (2004) Aquifer parameters estimation using artesian well test Data. *J Hydrol Eng* 9:64–67. [https://doi.org/10.1061/\(asce\)1084-0699\(2004\)9:1\(64\)](https://doi.org/10.1061/(asce)1084-0699(2004)9:1(64))
- Parkinson B, Spilker J (1996) Global Positioning System: Theory and Applications
- Perina T (2021) Flowing Well — time-domain solution and inverse problem revisited. *Groundwater* 59:438–442. <https://doi.org/10.1111/gwat.13064>
- Renard P (2005) Hydraulics of Well and Well Testing. *Encycl Hydrol Sci* 18. <https://doi.org/10.1002/0470848944>
- Renard P, Glenz D, Mejias M (2009) Understanding diagnostic plots for well-test interpretation. *Hydrogeol J* 17:589–600. <https://doi.org/10.1007/s10040-008-0392-0>
- Selles A (2014) Multi-disciplinary study on the hydrogeological behaviour of the eastern flank of the Merapi volcano, Central Java, Indonesia. Université Pierre et Marie Curie - Paris 6
- Selles A, Deffontaines B, Hendrayana H, Violette S (2015) The eastern flank of the Merapi volcano (Central Java, Indonesia): Architecture and implications of volcanoclastic deposits. *J Asian Earth Sci* 108:33–47. <https://doi.org/10.1016/j.jseae.2015.04.026>
- Singhal BBS, Gupta RP (2010) Applied hydrogeology of fractured rocks, Second edn. Springer, Dordrecht
- Sun X, Xu Y (2014) A hydraulic test device for free-flowing artesian boreholes with a case study in Table Mountain Group (TMG) aquifers, South Africa. *Water SA* 40:445–452. <https://doi.org/10.4314/wsa.v40i3.7>
- Sun X, Xu Y, Lin L (2015) The diagnostic plot analysis of artesian aquifers with case studies in Table Mountain Group of South Africa. *Hydrogeol J* 23:567–579. <https://doi.org/10.1007/s10040-014-1203-4>
- Swamee PK, Mishra GC, Chahar BR (2002) Simple approximation for flowing well problem. *J Irrig Drain Eng* 126:65–67. [https://doi.org/10.1061/\(asce\)0733-9437\(2000\)126:1\(65\)](https://doi.org/10.1061/(asce)0733-9437(2000)126:1(65))
- Thompson D (1929) Origin of artesian pressure. *Econ Geol* 24:758–771
- Todd DK, Mays LW (2005) Groundwater hydrology, 3rd editio. John Wiley & Sons
- Toulrier A, Baud B, de Montety V, Lachassagne P, Leonardi V, Pistre S, Dautria JM, Hendrayana H, Miftakhul Fajar MH, Satria Muhammad A, Beon O, Jourde H (2019) Multidisciplinary study with quantitative analysis of isotopic data for the assessment of recharge and functioning of volcanic aquifers: Case of Bromo-Tenger volcano, Indonesia. *J Hydrol Reg Stud* 26:100634. <https://doi.org/10.1016/j.ejrh.2019.100634>
- Trabucchi M, Carrera J, Fernández-García D (2018) Generalizing Agarwal's method for the interpretation of recovery tests under non-ideal conditions. *Water Resour Res* 54:6393–6407. <https://doi.org/10.1029/2018WR022684>
- Ungemach P, Bonnet M, Suzanne P (1968) Interprétation des essais de pompage en régime transitoire. Cas des mesures effectuées dans les puits. l'Effet de puits et la postproduction [Pumping tests interpretation in transient state. Measurements in the well. Bore-hole and post-production effects]. *Sci Géologiques, Bull mémoires* 21:325
- USGS (1996) Shuttle Radar Topography Mission (STRM), 1 arc-second for global coverage (~30 meters)
- Vasquez J (2010) Hydraulique Generale. Laboratoire Systèmes Hydrauliques Urbains - ENGEES
- Versluys J (1930) The origin of artesian pressure. *Econ Geol* 214–222
- Vuković M, Soro A (1992) Hydraulics of Water Wells: Theory and Application. Water Resources Publications
- Wang J, Jiang X-W, Wan L, Worman A, Wang H, Wang X, Li H (2015) An analytical study on artesian flow conditions in unconfined-aquifer drainage basins. *Water Resour Res* 8658–8667. <https://doi.org/10.1002/2015WR017104>
- Wendland E (2008) Friction loss correction in flowing well discharge tests. *Water Resour Res* 44:1–7. <https://doi.org/10.1029/2007WR006365>
- Wentworth CK (1951) Geology and ground-water resources of the Honolulu-Pearl Harbor area Oahu, Hawaii
- Willmann M, Carrera J, Sánchez-Vila X, Vázquez-Suñé E (2007) On the meaning of the transmissivity values obtained from recovery tests. *Hydrogeol J* 15:833–842. <https://doi.org/10.1007/s10040-006-0147-8>
- WMO, W. M. O, & UNESCO UNE and SO (2012) International glossary of hydrology. IHP/OHP-Berichte, Geneva
- Wyrick G, Floyd OE (1961) Microtime measurements in aquifer tests on open-hole artesian wells - method of aquifer tests. USGS Water-Supply Pap:1545-A 11

Publisher's note Springer Nature remains neutral with regard to jurisdictional claims in published maps and institutional affiliations.